Symmetry versus Commensurability: Epitaxial Growth of Hexagonal Boron Nitride on Pt(111) From B-Trichloroborazine $(ClBNH)_3$

Frank Müller,[†,‡] Klaus Stöwe,*[,†] and Hermann Sachdev*[,‡]

Institut für Analytische und Anorganische Chemie und Radiochemie and Institut für Anorganische Chemie FR 8.1, Universität des Saarlandes, Pf. 151150, 66041 Saarbrücken, Germany

Received August 17, 2004. Revised Manuscript Received February 8, 2005

The growth of hexagonal boron nitride (*h*-BN) on a Pt(111) surface by decomposition of B-trichloroborazine $(ClBNH)_3$ leads to two different sets of domain structures as indicated by low-energy electron diffraction (LEED). In addition to a domain structure, for which the top, hcp, and fcc sites of the substrate lattice are occupied by the BN lattice, there is a new type of domain structure with B and N alternatingly occupying the top and bridge sites of the Pt(111) substrate, a structural motif which has not been observed so far. The new domain structures are a result of the precursor chemistry (B-trichloroborazine vs borazine) as well as the lattice mismatch of the substrate [Pt(111) vs *h*-BN; mismatch ∼11%].

1. Introduction

The understanding of the nucleation phenomena and surface reactions of boron nitride phases on different substrates is of basic importance to develop and tune a phase-selective CVD process for hexagonal and cubic boron nitride. Ideal single-source precursors for the study of the primary reactions for the epitaxial growth of boron nitride phases are borazine $(HBNH)_3$, the BN analogous to benzene, and B-trichloroborazine $(ClBNH)_3$.

During recent years, the epitaxial growth of hexagonal boron nitride (*h*-BN) on transition metal surfaces, such as Ru(001), Pd(111), Pt(111), Ni(755), and Ni(111), has gained a lot of interest, and the electronic and the structural properties have been investigated by a large variety of surface-sensitive methods, as ARUPS, XPS, XPD, EELS, LEED, and STM.[1−7] Nagashima et al.[4] found that at the interface insulating *h*-BN is bound weaker to the metallic substrate crystal than its isostructural semimetallic counterpart graphite. They also reported that, following their procedure of preparing *h*-BN by the reaction of benzene-like $(HBNH)_3$ with (111) surfaces at high temperatures, it is possible to deposit exactly one monolayer of *h*-BN because the deposition rate drops strongly after the formation of the first layer. This possibility of a selective preparation of one *h*-BN monolayer as a two-dimensional quantum barrier makes the system *h*-BN/metal a promising tool for nanoelectronic or spintronic devices.[3,5] Furthermore, the primary reactions and film-forming mechanisms of boron nitride on different substrates are also of significant importance to understand the nucleation phenomena necessary for a phase-selective CVD process, e.g., the CVD of cubic boron nitride,[8−10] and are governed by the decay mechanisms and surface reactions of the precursors. The nature of the bond in sp^2- and sp^3-type BN phases is of a highly covalent character with ionic contributions due to the difference in electronegativity between boron and nitrogen atoms.

So far, most reports in the literature deal with the growth of *h*-BN on Ni(111) because the very small lattice mismatch of only 0.4% (a_{111}(Ni) = 0.249 nm, a(BN) = 0.250 nm) is easily compensated by a corrugation of the BN-lattice so that both lattices become commensurate.[1,5] Therefore, *h*-BN/Ni(111) represents an ideal system for the epitaxial growth of large, well-ordered *h*-BN domains.[3,5] The current research is focused on systems with a lattice mismatch between the substrate and *h*-BN as well as the influence of the precursor chemistry. Systems with a large lattice misfit between *h*-BN and the corresponding (111) substrate surface play a essential role in the formation of self-organized superstructures.[6,7] Recently, Osterwalder et al.[7] reported on the formation of a highly ordered self-organized two-monolayer nanomesh of *h*-BN grown on a Rh(111) surface with a lattice mismatch of about 7%. When the precursor chemistry is altered from borazine to B-trichloroborazine, both fcc- and hcp- type coverage on Ni(111) could be observed for the first time, although both forms differ only marginally in their energies.[3]

* To whom correspondence should be addressed. E- mail: h.sachdev@mx.uni-saarland.de; Fax: +49-681-302-3995; k.stoewe@mx.uni-saarland.de

† Institut für Analytische und Anorganische Chemie und Radiochemie,

‡ Institut für Anorganische Chemie FR 8.1, Universität des Saarlandes, Pf. 151150, 66041 Saarbrücken, Germany.

(1) Auwärter, W.; Kreutz, T. J.; Greber, T.; Osterwalder, J. *Surf. Sci.* **1999**, *429*, 229−236.
(2) Rokuta, E.; Hasegawa, Y.; Itoh, A.; Yamashita, K.; Tanaka, T.; Otani, S.; Oshima, C. *Surf. Sci.* **1999**, *427−428*, 97−101.
(3) Auwärter, W.; Suter, H. U.; Sachdev, H.; Greber, T. *Chem. Mater.* **2004**, *16*, 343−345.
(4) Nagashima, A.; Tejima, N.; Gamou, Y.; Kawai, T.; Oshima, C. *Surf. Sci.* **1996**, *357−358*, 307−311.
(5) Muntwiler, M.; Auwärter, W.; Baumberger, F.; Hoesch, M.; Greber, T.; Osterwalder, J. *Surf. Sci.* **2001**, *472*, 125−132.
(6) Paffet, M. T.; Simonson, R. J.; Papin, P.; Paine, R. T. *Surf. Sci.* **1990**, *232*, 286−296.
(7) Corso, M.; Auwärter, W.; Muntwiler, M.; Tamai, A.; Greber, T.; Osterwalder, J. *Science* **2004**, *303*, 217−220.
(8) Sachdev, H.; Strauss, M. *Diamond Relat. Mater.* **2000**, *9*, 614−619.
(9) Sachdev, H. *Diamond Relat. Mater.* **2001**, *10*, 1390−1397.
(10) Sachdev, H. *Diamond Relat. Mater.* **2003**, *12*, 1275−1286.

10.1021/cm048629e CCC: $30.25
Published on Web 05/28/2005

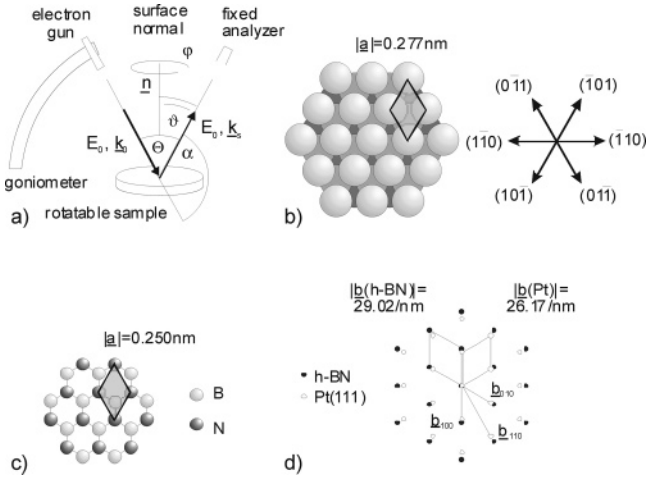

Figure 1. (a) Experimental setup, (b) lattice structure of Pt(111) with the directions referring to the surface normal being along (111), (c) lattice structure of one monolayer of *h*-BN, and (d) reciprocal surface lattices of Pt(111) and *h*-BN.

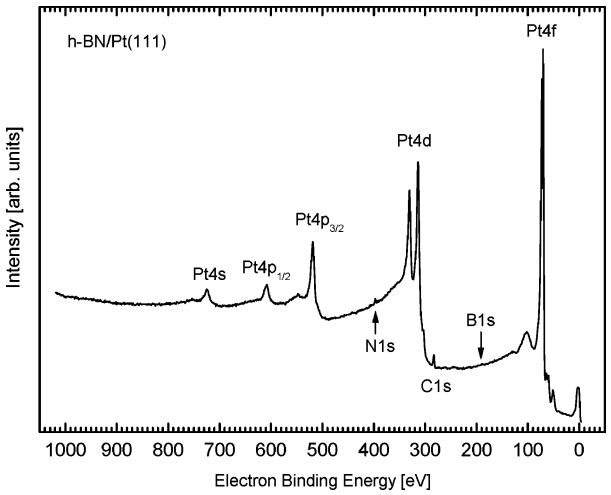

Figure 2. XPSpectrum of 40 L *h*-BN on Pt(111). Besides the substrate signal, only the N 1s and a small C 1s intensity can be detected. The cross section for B 1s is too small to give a distinct signal for one monolayer *h*-BN.

An important question is now how a modified precursor chemistry affects the BN formation on systems with a large lattice misfit. Therefore, LEED investigations on the epitaxial growth of *h*-BN monolayers on Pt(111), a system with a lattice mismatch of approximately 11% (a_{111}(Pt) = 0.277 nm), from B-trichloroborazine as precursor, were performed in order to find out if there are differences in the resulting domain structures compared to those found for one-monolayer *h*-BN/Ni(111), a system with a nearly vanishing misfit[3,5] as well as borazine as precursor.[6]

2. Experimental Section

Experimental Setup. The experimental setup is described in detail in previous papers.[11−13] The experiments were performed with a modified VG ESCA MkII spectrometer, which is especially designed for X-ray photoelectron diffraction (XPD) as well as for low-energy electron diffraction (LEED, AREELS) investigations. The core component consists of an Osterwalder-type manipulator with two rotational degrees of freedom, which allows the hemispherical energy analyzer to detect the electrons within the full 2π hemisphere above the surface of the sample. In LEED, the scattering angle α between the electron gun (ΔE = 200 meV at E_0 = 50 eV and I_{em} = 5 nA) and the analyzer is fixed, while the sample is tilted stepwise by the polar angle ϑ. At each ϑ, the sample is additionally rotated around its surface normal by the azimuth angle φ in the full 2π range, as depicted in Figure 1a. A hemispherical LEED pattern is usually used only for a qualitative interpretation of the surface structures. It typically consists of about 10000−20000 angular settings, which are recorded within about 1−2 h. For a quantitative analysis, additional polar intensity plots can be recorded along the high-symmetry directions with reduced angular step widths. Hemispherical LEED patterns as well as polar intensity plots are originally recorded as $I(\vartheta,\varphi)$ or $I(\vartheta,\varphi$ = const.) plots, respectively. They can be transformed into the more common $I(\Delta q||)$ plots via

$$\Delta q|| \,[\mathrm{nm}^{-1}] = 20 \times 0.512 \times \sqrt{E_0[\mathrm{eV}]}\,\cos(\Theta/2)\,\sin(\vartheta - \Theta/2)$$

for Θ (cf. Figure 1a). Figure 1 gives also a survey about the lattice structures of Pt(111) and *h*-BN in real and in reciprocal space, the corresponding lattice constants, and the definition of the symmetry directions.

Preparation of the BN Films. The Pt(111) substrate crystal was cleaned in several cycles of Ar ion sputtering (up to 4 keV) and subsequent annealing (up to 1000 K). Because the crystal was in use for the first time, sputtering as well as annealing was started for several hours and the periods of these processes were reduced with each step of preparation, until in XPS the C 1s and O 1s contaminations were beyond the detection limit and until the LEED patterns exhibited sharp spots. The preparation of the BN films was similar to the procedure described in ref 4, i.e., the temperature of the Pt(111) crystal was set to 1000 K, but instead of benzene like borazine $(HBNH)_3$, B-trichloroborazine $(ClBNH)_3$ was used as described in ref 3. B-trichloroborazine $(ClBNH)_3$, twice refined by sublimation, was inserted into a Schlenk tube within an Ar atmosphere. The glass tube had a metal KF flange attached and could be evacuated via a turbomolecular pump down to 10^{-6} mbar. The precursor was additionally purified by several cycles of heating to 350 K and subsequent evacuating of the glass tube, as described in ref 3. Then, $(ClBNH)_3$ was put into the preparation chamber via the Ar gas inlet of the sputter gun, while all parts of the spectrometer that the precursor had to pass were being kept at 350 K. During the deposition, the pressure was 5×10^{-7} mbar for about 120 s, resulting in a nominal deposition dose of 48 L.

3. Results and Discussion

Figure 2 shows the normal emission XPSpectrum (Al Kα excitation at E = 1485 eV) of the Pt(111) crystal after the deposition of $(ClBNH)_3$. Compared to the spectrum of the clean Pt(111) surface, the spectrum additionally exhibits a slight C 1s intensity (arising from adventitious background species in the dosing line or chamber, and not from the quality of the precursor[3]), while due to their small cross sections, the N 1s and B 1s intensities are hardly or not visible. The upper limit of the actual thickness of the BN film can be set to one monolayer because from the growth of BN on Pt(111), Ni(111), and Pd(111) surfaces it is known that the growth rate strongly drops after the formation of

(11) Müller, F.; Steiner, P.; Straub, T.; Reinicke, D.; Palm, S.; de Masi, R.; Hüfner, S. *Surf. Sci.* **1999**, *442*, 485−497.
(12) Müller, F.; de Masi, R.; Steiner, P.; Reinicke, D.; Stadtfeld, M.; Hüfner, S. *Surf. Sci.* **2000**, *459*, 161−172.
(13) Müller, F.; de Masi, R.; Reinicke, D.; Steiner, P.; Hüfner, S.; Stöwe, K. *Surf. Sci.* **2002**, *520*, 158−172.

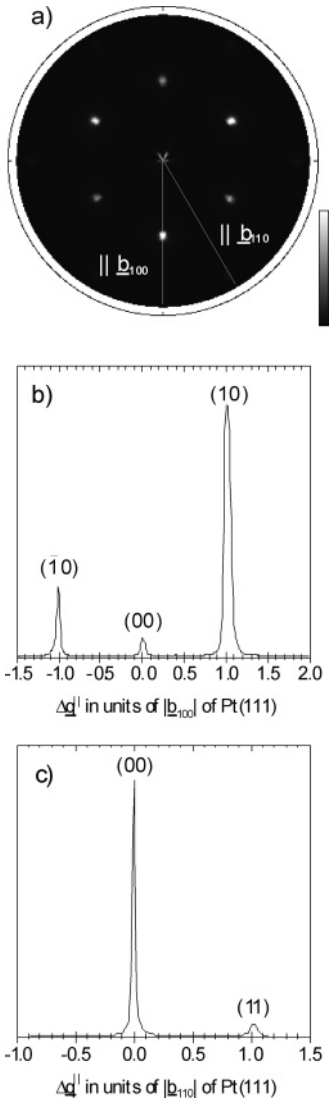

Figure 3. (a) LEED pattern ($E_0 = 50$ eV, $\alpha = 120°$) of the clean Pt(111) surface. (b) Polar intensity plot along the b_{100} direction (corresponds to $(11\bar{2})$ direction in real space). (c) Polar intensity plot along the b_{110} direction (corresponds to $(01\bar{1})$ direction in real space).

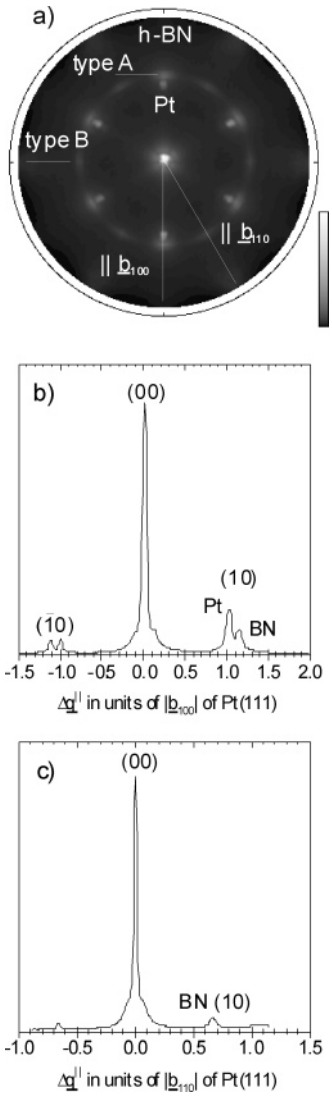

Figure 4. (a) LEED pattern ($E_0 = 50$ eV, $\alpha = 120°$) of less than or equal to one monolayer *h*-BN/Pt(111) surface with two additional sets of hexagonal intensity distributions. (b) Polar intensity plot along the b_{100} direction. The (10) spot splits into the Pt(111) and *h*-BN contributions with $|b_{100}(h\text{-BN})| \approx 1.11|b_{100}(\text{Pt})|$, according to the 11% lattice mismatch. (c) Polar intensity plot along the b_{110} direction with a spot at $0.65|b_{110}(\text{Pt})|$, which is equal to $0.64\sqrt{3}|b_{100}(\text{Pt})| = 1.12|b_{100}(\text{Pt})| \approx |b_{100}(h\text{-BN})|$, i.e., the BN lattice of (b) is additionally rotated by 30°.

the first monolayer,[3,4] and furthermore, the nominal deposition dose of 48 L is in the same range as that reported in ref 1, where the analysis of the XPS intensities of a BN/Ni(111) system results in a BN coverage of one monolayer.

Figure 3 shows the LEED pattern of the clean Pt(111) surface, as well as the corresponding polar intensity plots along the reciprocal (100) and (110) directions (as defined in Figure 1d). The LEED pattern was recorded at $E_0 = 50$ eV, i.e., at a primary energy, at which, following the "universal" curve for electron attenuation, the surface sensitivity is at its maximum. But despite the high surface sensitivity, the pattern exhibits sharp spots of 3-fold instead of 6-fold symmetry, indicating that the discrimination between the different fcc sites of the second and third layers has to be taken into account.[3,5]

After the deposition of 48 L B-trichloroborazine the intensity distribution of the LEED pattern changes into that depicted in Figure 4a. The LEED pattern exhibits additional spots which are nearly as sharp as in the case of the clean Pt(111) surface, indicating that *h*-BN forms large well-ordered domains. The most prominent features of the LEED pattern are the double structures arising from the Pt and *h*-BN spots, which are separated by about 10% in accordance with the lattice mismatch of 11%. Due to this lattice mismatch, an isosymmetrical epitaxial growth (i.e., the symmetry of the *h*-BN film is the same as that of the Pt substrate) would result in a 9×9 superstructure (SS) with respect to the Pt(111) lattice. This superstructure causes the distinct hexagonal spot arrangement around the (00) reflex as well as the additional spot, which can be attributed to the $(n/9,m/9)$ reflexes (cf. Also the high-resolution polar intensity plots in Figure 4b and Figure 4c along the b_{100} and b_{110} directions).

These isosymmetrical domain structures (type A), which were also observed for the growth of BN/Ni(111) in refs 1, 3, and 5, have in common that the symmetry of the *h*-BN layer is adapted to that of the metallic substrate (in the case of *h*-BN/Ni(111), the adaption of symmetry is even in accordance with commensurability due to the small lattice mismatch of about 0.4%). Type A domains can be further

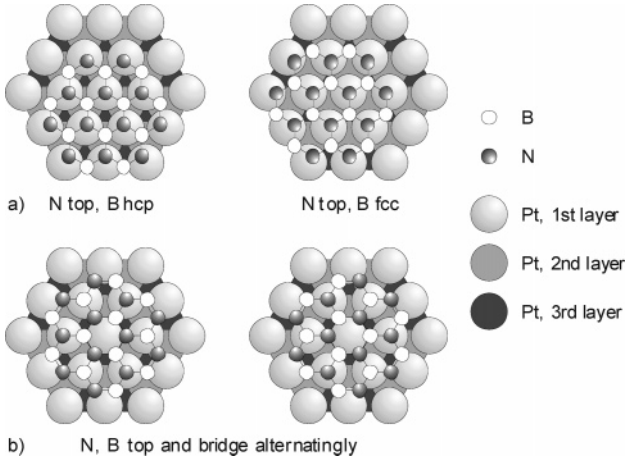

Figure 5. (a) A-type domain structure of *h*-BN/Pt(111), with, e.g., N on top and B on hcp (left) or B on fcc site (right), as proposed for *h*-BN/Ni-(111). (b) B-type domain structure with B and N on top and bridge sites.

divided in A′, A″, ... types (cf. Figure 1 in ref 5 or Figure 3 in ref 3), depending on the actual positions of the B and N atoms, i.e., top, hcp, or fcc site, cf. Figure 5a. These A type domains differ only by the adsorption sites of the B and the N sublattices, while the absolute orientation of the B and N sublattices with respect to the substrate lattice is the same; i.e., the LEED patterns of A type domains always have the same orientation as that of the (111) substrate.

But for BN/Pt(111), it is even the large lattice mismatch that causes the BN lattice to form a new type of domains, namely, B-type, which is indicated by the miscolored gray scale plot of the LEED pattern in Figure 4a as well as by the polar intensity plot along the b_{110} direction in Figure 4c. The additional spots in Figure 4c correspond to a transfer of momentum of about $0.64b_{110}$(Pt), which is equal to $0.64\sqrt{3}b_{100}$(Pt) $= 1.1b_{100}$(Pt) $= b_{100}$(BN), i.e., the *h*-BN lattice is rotated by 30° with respect to the A-type domains.

The reduction of the lattice parameter of about 11% causes the diameter of the B_3N_3 ring, i.e., the distance of opposite B and N atoms, to deviate only by about 4% from the lattice constant of Pt(111). Therefore, the observed B-type domains, which are rotated by 30% with respect to the A-type domains, result from such a growth mode, for which the B and N atoms occupy alternatingly the top and bridge sites of the substrate lattice, as depicted in Figure 5b. The B-type domains can therefore be considered as surface structures that are closer to commensurability to the substrate lattice than the A-type domains. These structures were not observed for borazine, whereas the chlorinated system enables the formation of the additional type "B"-domains.[6] Since ring-opening mechanisms are considered in the growth of *h*-BN monolayers on Ni(111) from borazine and B-trichloroborazine, differences in the desorption behavior from specific surface sites of additional cleavage products (hydrogen in the case of borazine, hydrogenchloride in the case of B-trichloroborazine) may be considered as the cause for the formation of additional domain structures.

From the present results, the growth of *h*-BN on Pt(111) seems to be determined by two driving forces, i.e., symmetry vs commensurability. On one hand, the orientation of the BN lattice is adapted to the symmetry of the Pt(111) surface (A-type domains). On the other hand, the BN lattice attempts to adapt the periodicity of the substrate lattice by forming the superstructures of the B-type domains by reducing the point symmetry. From inspection of the ratio of the intensity contributions from both domain types in Figure 4, the relative weight is strongly shifted toward the A-type domains; i.e., the adaptation of symmetry may be a more decisive factor than the adaptation of periodicity. To find out whether the symmetry plays indeed such an important role, future investigations have to be extended to such systems that have a large mismatch with respect to the A-type domains, but a smaller mismatch with respect to the B-type domains, as, e.g., Au(111) or Ag(111). For both substrates, the *h*-BN lattice deviates less than 10^{-3} from the commensurability with the substrate lattice for B-type domains, while the deviation for A-type domains is larger than 13%. Furthermore, it is necessary to investigate the additional domain structures of *h*-BN on Pt(111), as supported by the presented results, which are based on reciprocal space data, also in real space, e.g., by STM or XPD investigations.

4. Summary

The growth of *h*-BN on Pt(111) from B-trichloroborazine leads to the formation of new domain structures, which so far have not been observed for systems with a very small lattice mismatch like *h*-BN/Ni(111). The presented results clearly demonstrate that a variation of the precursor chemistry significantly influences the resulting superstructures on the metal surface since the presented superstructures were not observed for borazine/Pt(111). In addition to BN− domains, for which the orientation of the B and N sublattices coincide with that of the Pt(111) substrate (A-type), BN also forms domains, for which the B and N sublattices are rotated by 30° with respect to the Pt(111) substrate (B-type). In the first case, the BN lattice adapts the symmetry of the substrate lattice at the cost of a poor lattice mismatch, while in the second case, the lattice mismatch is reduced by more than 60% at the cost of the loss of symmetry. From inspecting the intensity contributions of both domain types, the conservation of symmetry seems to be more decisive than the adaptation of a common periodicity.

Therefore, the growth of *h*-BN monolayers on Ag(111) or Au(111) surfaces shall be characterized because, for these substrates, there is nearly no lattice mismatch for B-type domains, while the lattice mismatch of A-type domains is still larger than that for Pt(111), and also the influence of single-source precursors delivering only one BN− formula unit per molecule instead of three formula units, as is the case for borazine-derived compounds, shall be studied to obtain more knowledge of the surface reactions regarding the formation of boron nitride films.

Acknowledgment. This work was supported by the Deutsche Forschungsgemeinschaft within the project Synthesis of superhard Materials and Reactivity of Solids and by the Fonds der Chemischen Industrie. The authors especially thank S. Hüfner for providing the experimental equipment.

CM048629E